Wiley Online Library
Early View publication on www.wileyonlinelibrary.com
(issue and page numbers not yet assigned;
citable using Digital Object Identifier – **DOI**)

J. Biophotonics 1–8 (2017) / **DOI** 10.1002/jbio.201600318

Journal of BIOPHOTONICS

FULL ARTICLE

Alzheimer mouse brain tissue measured by time resolved fluorescence spectroscopy using single- and multi-photon excitation of label free native molecules

Bidyut Das[+],[1] *Lingyan Shi*[+],[2,3,4] *Yury Budansky*,[2] *Adrian Rodriguez-Contreras*,[2,3] *and Robert Alfano*[*,2]

[1] Department of Physics, Fairfield University, Fairfield, CT 06824, USA
[2] Institute for Ultrafast Spectroscopy and Lasers, Department of Physics, the City College of New York, New York, NY 10031, USA
[3] Department of Biology, the City College of New York, New York, NY 10031, USA
[4] Department of Chemistry, Columbia University, New York, NY 10027, USA

Received 14 February 2017, revised 1 March 2017, accepted 10 March 2017

Keywords: Alzheimer disease, time resolved fluorescence spectroscopy, label free molecule, multiphoton excitation, brain optics

Time resolved spectroscopic measurements with single-photon and multi-photon excitation of native molecules were performed *ex vivo* on brain tissues from an Alzheimer's disease (AD) and a wild type (WT) mouse model using a streak camera. The fluorescence decay times of native NADH and FAD show a longer relaxation time in AD than in WT tissue, suggesting less non-radiative processes in AD. The longer emission time of AD may be attributed to the coupling of the key native building block molecules to the amyloid-tau and/or to the caging of the native fluorophores by the deposition of amyloid-beta or tau plaques and neurofibrillary tangles that affect the local non-radiative interactions.

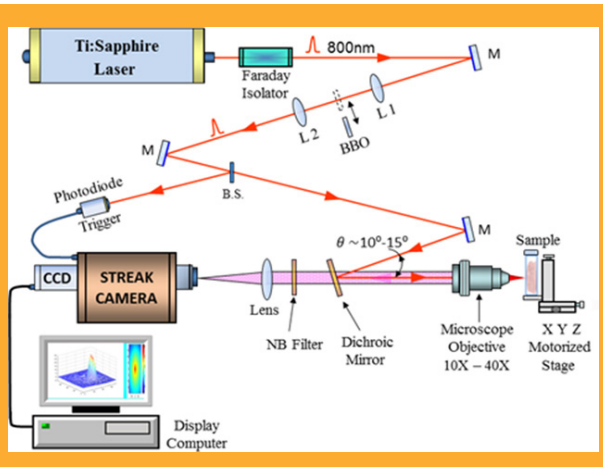

1. Introduction

Alzheimer's disease (AD) attacks neurons in the brain and leads to the loss of proper cognition, but there is no molecular understanding of the processes involved. Early diagnosis can help people make better decisions for the future while they are still capable, and can allow them to receive early treatment to improve their cognition and the quality of their lives as they live with AD. Methods of diagnosis of AD include use of Magnetic Resonance Imaging (MRI) to look for Hippocampal atrophy, Positron Emission Tomography (PET) scans, and examining levels of amyloid-beta and tau protein in cerebrospinal fluids taken from the patient [1]. Photonics methods offer new and novel approaches to obtain molecular information on the onset and progress of AD. The use of optical spectroscopy to detect

* Corresponding author: e-mail: ralfano@ccny.cuny.edu
[+] B. Das and L. Shi equally contributed to this work.

disease on a molecular level offers a way to probe brain tissue by examining the fluorescence levels of native key organic biomolecules in tissues. Native fluorescence of proteins and molecules in human tissue has been used in the past to examine levels of tryptophan, nicotinamide adenine dinucleotide hydrate (NADH), flavin, and collagen in normal and cancerous breast tissue for diagnosing certain types of cancer [2–4]. Fluorescence lifetime measurements for cancer detection targeting NADH, flavin adenine dinucleotide (FAD) and various other label free native molecules by many different groups using animal and human tissue from different body parts are discussed elsewhere [2–6].

Tryptophan kynurenine metabolism has been reported to be involved in the pathogenesis of AD [7]. Change of NADH-linked mitochondrial enzymes has been found in AD brain [8]. It is well known that neuro-degeneration associated with AD points to the extracellular aggregates of amyloid-β (Aβ) plaques and tangles as the neuropathological markers of this age-related disease [9]. Neurotoxic inflammation and neuronal death from disrupted cellular activities and communication in the brain has been shown to be associated with the deposition of Aβ-plaques [10,11]. Aβ-plaques destroy synapses before it begins to clump into plaque, which initiates the deterioration in brain function [12].

It has been shown recently that the onset of Amyloid build-up can start decades before the clinical signs of dementia appear [13–15]. Amyloid deposits and tangles are accompanied by a marked loss of neurons in the neo-cortex and hippocampus. The definitive diagnosis of AD is currently possible by detecting these amyloid-β plaques after brain autopsy. During the development of *in vivo* amyloid imaging agents, it has been shown that binding of the positron emission tomography tracer Pittsburgh Compound-B reflects the amount of Aβ in AD brain but not in transgenic mouse brain [16].

In an attempt to develop alternative noninvasive detection modalities, optical imaging of AD by monitoring Aβ plaques in the retina as an extension of the brain has been achieved [17]. It was shown that an immune-based therapy effective in reducing brain plaques significantly reduced retinal Aβ plaque burden in immunized versus non-immunized AD mice. Based on the parallel growth of Aβ plaques on eye lens diagnostic methods are being developed by using amyloid-binding fluorescent ligand Aftobetin [13].

In order to achieve deep brain imaging our group has explored four optical tissue windows recently with single- and multi-photon excitation in the near-infrared (NIR) region [18]. Lifetime of intrinsic fluorescence, which develops during the aggregation of a range of polypeptides, including the disease-related human peptides amyloid-β (1–40) and (1–42), lysozyme and tau has been reported in the nano second regime by using time correlated single photon counting fluorescence lifetime imaging (TCSPC-FLIM) [19].

The focus of this study is for the first time to use single-photon (1P) and multi-photon excitation and high resolution (10 ps) time resolved fluorescence spectroscopy for measuring the relaxation kinetics of key biomolecules (tryptophan, NADH, and Flavins) in AD and wild type (WT) mouse brain tissues, and to propose a potential method for better understanding and detection of AD and energy flow pathways in the brain. Single-photon and multi-photon excitation of these label-free molecules are used to probe morphological changes occurring in the brain tissue of an AD mouse by directly measuring time-resolved fluorescence decay using a Streak camera with 10-ps time-resolution [4]. Two-photon (2P) and three-photon (3P) excitation are non-linear optical processes achieved with higher order electric fields of femtosecond (fs) laser pulses. Time-resolved spectroscopic techniques can help isolate participating fluorophores. Study of the relaxation time can provide information on the heterogeneous nature of fluorescence, the environmental changes around the fluorophore and the non-radiative processes involved [4]. These findings of AD fingerprints in our direct temporal fluorescence study of the mouse model are presented here for the first time.

2. Materials and Methods

2.1 Brain tissue preparation

Mice were purchased from The Jackson Laboratory and housed at the City College Animal Facility. An 8-month-old triple transgenic AD mouse harboring PS1M146 V, APPSwe, and tauP301 L transgenes in a uniform strain background [20] was used. Another WT mouse at the same age was used as control. The experimental procedures were approved by the Institutional Animal Care and Use Committee of the City College of New York.

After anesthesia with a mixture of ketamine and xylazine (41.7 and 2.5 mg/kg body weight, respectively), the mouse was decapitated and the brain was dissected and taken out. Brain tissue with the hippocampus region was quickly sliced coronally at thickness of ~2 mm (Figure 1) with a brain matrix (RWD Life Science Inc., CA). The fresh brain tissue slice was then immediately placed on a glass slide. Regions of interest (ROI) in the hippocampus were

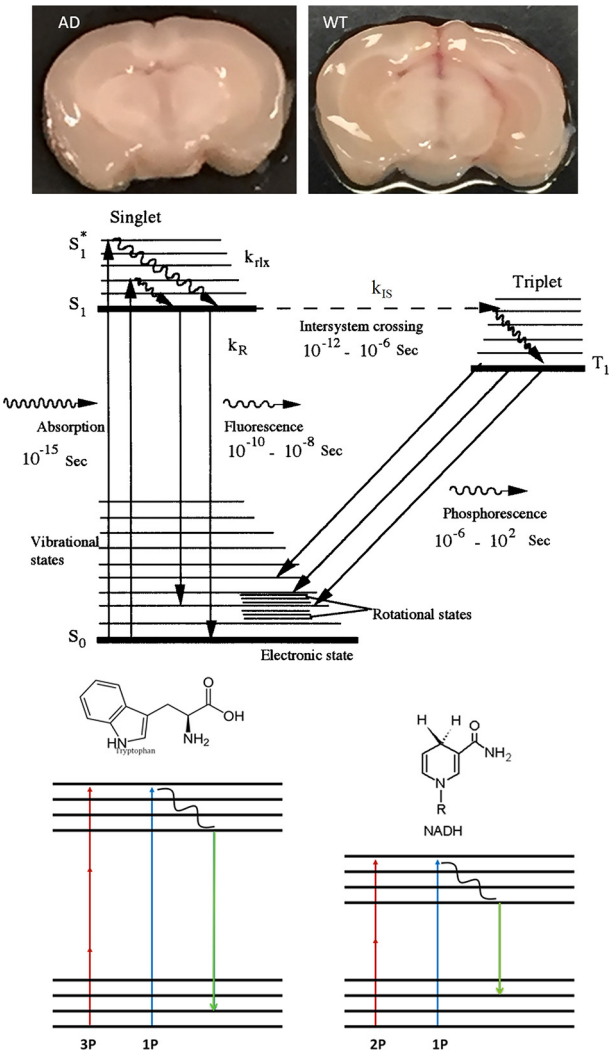

Figure 1 1a. Brain slice from mice of Alzheimer's disease (AD) model and wild type (WT). **1b.** Photo-physics processes in a simplified energy level diagram of a polyatomic organic molecule. Figure **1c.** Simplified energy level diagram for single-photon (1P), two-photon (2P) and three-photon (3P) excitation processes.

measured 3 times at different spots in each AD and WT brain slice (Figure 1a).

2.2 Model of photoexcitation and fluorescence molecular relaxation

Figure 1 illustrates the optical physics of a molecule excited by short pulses decaying to the ground state while undergoing various radiative and non-radiative processes. The excited molecule quickly relaxes through the vibrational levels to populate the lowest level of the excited state. The molecule then comes down to the ground state by losing energy through emission of fluorescence as well as through various non-radiative processes. The probability of radiation transition per second is given by the decay rate constant, k_R, while the non-radiative process is described by the constant, k_{NR}. The non-radiative process includes *internal conversion* (k_{IC}) through vibrational relaxation, collision by diffusion and rotational motion, and coupling with the environment, *intersystem crossing* from singlet to triplet states (k_{IS}), and *quenching* (k_q) of fluorescence by other molecules. The fluorescence decay time (τ_F) is given by the reciprocal of the fluorescence decay constant k_F, such that:

$$1/\tau_F = k_F = k_R + k_{NR} = k_R + (k_{IC} + k_{IS} + k_q) \quad (1)$$

The fluorescence intensity $I(t)$ is given as a function of time as follows [4]:

$$I(t) = k_R n_{S1}(t) \quad (2)$$

where $n_{SI}(t)$ is the population of molecules at the bottom of the vibrational levels of the excited state S_1. This population has been shown to have the following form involving the initial photon number of the incident delta-function laser pulse n_0, the relaxation rate k_{rlx}, and the fluorescence decay rate k_F:

$$n_{S1}(t) = \frac{k_{rlx} n_0}{k_{rlx} - k_F}(e^{-k_F t} - e^{-k_{rlx} t}) \quad (3)$$

The rise time of the time-resolved fluorescence emission profile is associated with the time to reach the emitting state, and it gives a measure of the vibrational thermalization for excitation states to be populated; while the fluorescence decay time gives information on interactions between the molecules and the host, giving rise to intersystem crossing and internal conversion. The non-radiative relaxation rate determines the life time of the fluorescence. Restrictive motion causes less non radiative pathways and longer lifetime. Critical optical properties of a Gaussian laser beam in two-photon or multi-photon fluorescence imaging have been theoretically analyzed in ref [21,22].

2.3 Multi-photon time resolved experimental setup

Figure 2 displays the experimental setup for the single- and multi-photon time-resolved fluorescence spectroscopy measurement. A Coherent Mira 900 Mode-locked Ti : Sapphire laser was used to generate 100 fs laser pulses at wavelength 800 nm and repetition rate 82 MHz. A BBO crystal was inserted

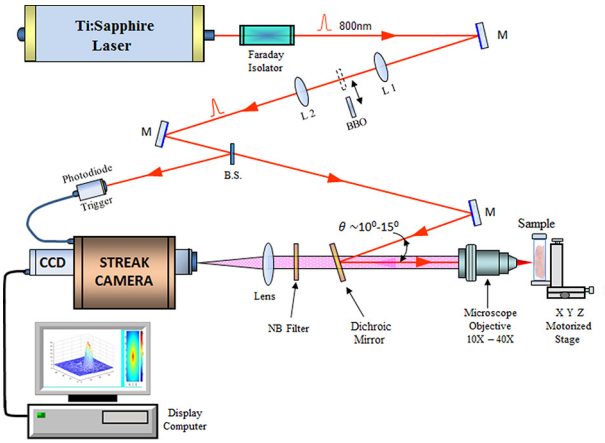

Figure 2 The experimental setup for the single- and multi-photon time-resolved fluorescence spectroscopy measurements.

into the beam to generate the second-harmonic at 400 nm. A dichroic mirror and a microscopic objective were used to focus the *fs*-laser pulses with ~120 mW power at the sample resulting in ~1.46 nJ of energy per pulse. As shown in Figure 2, the front surface of the brain tissue sample was excited with 800 nm and 400 nm pulses with a spot size of about 100 μm and a depth of about 0.5 mm. The resulting fluorescence from NADH, FAD and tryptophan, passing through a dichroic mirror and narrowband (NB) filters appropriate for the desired emission band, was focused onto the slits of a Hamamatsu synchro-scan streak camera with a 10-ps time-resolution [4].The temporal emission signal was obtained by averaging 82 MHz laser pulses using the streak camera in a synchroscan mode operation. In order to improve the signal-to-noise ratio the emission was integrated over a period of 10 to 60 seconds. The

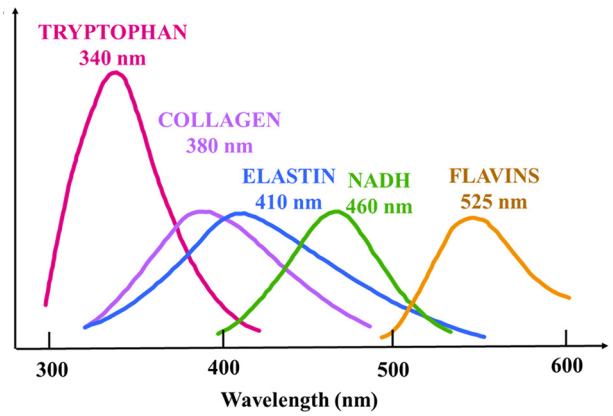

Figure 3 Emission spectra of several label free molecules [3].

sample mounted on a micrometer translation stage was moved to excite different parts of the hippocampus regions. This method of using time-resolved synchroscan streak mode enables one to achieve a dynamic range of over 10,000 for the bio samples with low fluorescence yield.

Figure 3 is based on our previous work [3] and displays the emission curves from key native fluorophores. Single-photon excitation was performed with 400 nm light while 2P and 3P excitation were achieved with 800 nm pulses. The emission was collected with a 440 ± 25 nm NB filter for NADH which has an emission peak around 460 nm. The signal for FAD with an emission peak around 525 nm was collected with a 530 ± 25 nm NB filter. A 340 ± 25 nm NB filter was used to collect the 3P-fluorescence emission from tryptophan with excitation at 800 nm. The time-resolved intensity profiles were fitted to a double exponential decay function below using the least square method:

$$y = y_0 + a_1 e^{-t/t_1} + a_2 e^{-t/t_2} \quad (4)$$

The short and the long decay times, t_1 and t_2, were found by fitting these experimental curves.

3. Results

3.1 *Single-photon absorption time-resolved fluorescence*

Figure 4 displays time-resolved fluorescence intensity profiles from AD (black) and WT brain tis-

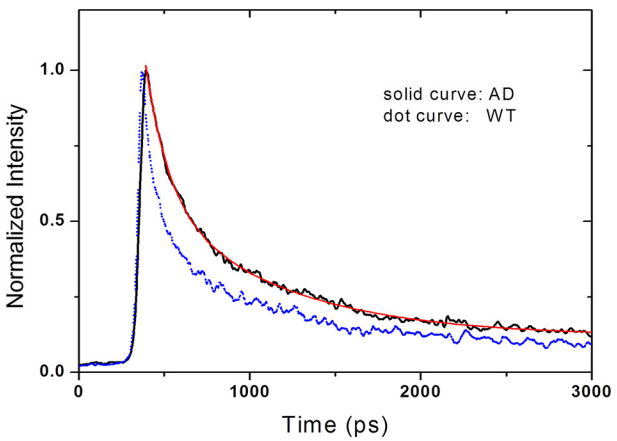

Figure 4 Time-resolved intensity profiles of flavins (FAD) from AD and WT mouse brain tissue at 400 nm excitation and 530 nm emission. Both the fast and the slower decay times from AD tissues are almost double compared to the decay times from WT brain.

sue (blue) samples excited at 400 nm pulses. These two typical profiles highlight the significant difference in the decay time, with the AD sample showing much longer decay. The red curve is the theoretical fit to the AD profile.

The time-resolved measurements were performed on various points on two normal and two AD samples (hippocampus). The double exponential fitting results are listed in Table 1. The decay has a fast component with a shorter lifetime (t_1) and a slow component with a longer lifetime (t_2). The emission at 440 nm and 530 nm from NADH and FAD respectively show huge differences in t_1 and t_2 between AD and WT tissues, showing a clear signature of AD for diagnostic and imaging purpose. In order to see the relative contribution of the fast and slow decay processes, the last column in Table 1 displays the ratio of the amplitudes of the two decay components.

Our measurements of the slower component of the lifetime compare well with the measurements from other groups. Many groups using multi-photon imaging with time-correlated single photon counting have reported fluorescence life times mostly in nano-second regime because of lower time resolution of their system or longer pulse widths [23–26]. One group using time-correlated single photon counting and along with a custom algorithm, found three distinct lifetime peaks for rat hippocampus and human cortex [24]. The peak with the greatest amplitude occurred around 200 ps–450 ps (rat and human). A second peak with medium amplitude occurred around 450 ps–800 ps, while a peak with small amplitude appeared at lifetimes ranging from 3 ns–6 ns. Another group using FLIM measurement on human normal cortex found a lifetime of 1280 ps clearly limited by the 500 ps time-gate and a 700 ps nitrogen pulse laser [25,26].

Though these groups and others have measured NADH/NADPH life-times that are close to our measurement of the slower component, no one to our knowledge has measured a component shorter than 100 ps that bears the signature of AD. This is due to the superior 10ps time resolution of the streak camera that directly measures the time-resolved fluorescence intensity profiles. This fast component, which is the dominant one between the two, as seen from the last column with the amplitude ratios is also critical for separating AD from normal brain tissue.

3.2 *Multiphoton time resolved fluorescence*

Figure 5 displays the normalized time-resolved fluorescence intensity profiles from NADH. The excitation wavelengths were 400 nm and 800 nm, respectively, for 1P and 2P, and emission wavelength 440 nm for both. The relaxation time for two photon excitation fluorescence (2PEF) is faster than the 1PEF even though the molecules are photo excited to the same energy state higher by 3.1 eV. This difference is explained in the Discussion section.

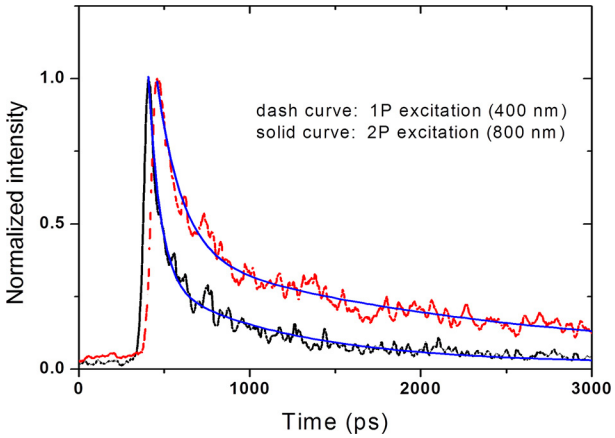

Figure 5 Time-resolved fluorescence intensity profiles (normalized) of NADH from an AD hippocampus tissue. Excitation wavelengths were 400 nm and 800 nm respectively, with emission at 440 nm. The smooth lines are the theoretical fits.

Figure 6 displays the normalized fluorescence emission from tryptophan in the AD tissue excited by 3P. The fluorescence decay time has a single exponential decay of 240 ps. This recording of rare time-resolved three-photon fluorescence emission opens up possibilities of three-photon imaging of tryptophan in brain as an Alzheimer's signature.

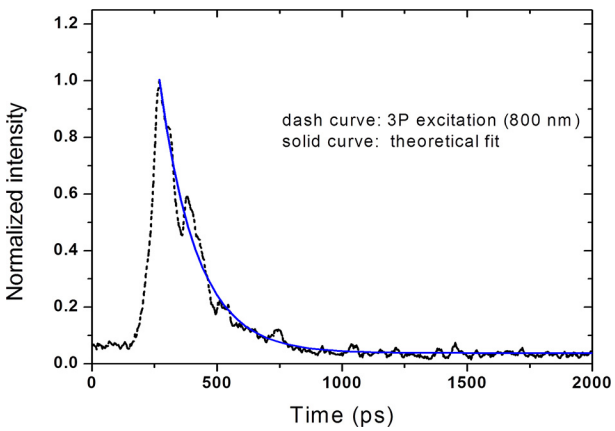

Figure 6 Time-resolved 3P fluorescence intensity profiles from tryptophan in an AD brain tissue excited at 800 nm with emission at 340 nm.

Table 1 Fluorescence lifetime in AD and WT brain tissues using single photon excitation. Excitation wavelength is 400 nm.

Molecule	Sample	Emission (nm)	t_1 (ps)	t_2 (ps)	a_1/a_2
NADH	AD	440	86.0 ± 20.2	706.5 ± 21.4	232.8
	WT	440	26.8 ± 13.1	527.2 ± 102.7	300
FAD	AD	530	95.7 ± 27.4	722.3 ± 60.6	122.0
	WT	530	56.4 ± 19.6	584.0 ± 100.1	136.2

Table 2 summarizes fluorescence lifetimes and their relative strengths from single- and multi-photon excitation of NADH, FAD and tryptophan in AD tissue. The profiles from single- and two-photon excitation show a double exponential decay with a shorter (t_1) and a longer (t_2) life-time component. The emission from 2P excitation at 800 nm shows a much faster decay compared to emission from 1P excitation at 400 nm for both NADH and FAD. Both components of fluorescence lifetimes from 1P excitation are much longer compared to the lifetimes from 2P excitation. Another group has measured NADH 2P lifetimes (emission: 350–550 nm) in hippocampal slices from Sprague-Dawley rats using time-correlated single photon counting, and has found four different lifetimes: 155 ps, 599 ps, 2.2 ns and 6 ns [27]. Keeping in mind the lower time resolution of this photon counting method, our measurements compare well with the first two lifetimes, while the investigation of the other two longer lifetimes is not part of our study.

The emission at 340 nm is most likely from tryptophan with 3P excitation. The time-resolved 3P measurement on a single brain tissue sample is given as a proof-of-principle on the feasibility of exciting tryptophan with three photons. More 3P measurements are needed to explore its diagnostic potential.

4. Discussion

The differences in fluorescence lifetimes as seen above suggest that environmental and possible structural changes in AD tissue affect the fluorescence profile of key metabolic molecules FAD and NADH. The longer fluorescence lifetime of AD tissue shows less non-radiative decay that may occur once amyloid-β (Aβ) plaques are formed. We assume that this is most likely due to the restricted motion of the fluorophore, which is bound to the plaques, reducing the non-radiative pathways for relaxation and resulting in a longer lifetime. Non-radiative decay processes occur due to collision by diffusion, energy transfer with fast rotational motion of the molecules and/or quenching of emission by other species while the molecules relax to the ground state. Another group has shown that by adding the enzyme malate dehydrogenase (MDH) to a solution of unbound NADH, the lifetime increased from 480 ps to 769 ps. This showed that MDH (non-fluorescent) was binding to NADH (fluorescent) and thereby resulting in an increase of its fluorescence lifetime [24]. Previous work using amyloid-binding ligands where an ointment was administered into the eye has shown similar reduction in non-radiative processes and increase in ligand lifetime when the extrinsic ligand binds to Aβ plaques [12]. This binding most likely reduces the diffusion and rotational motion resulting in a decrease of the number of channels for transferring energy. This suggests that the longer lifetime in our AD sample is due to reduced non-radiative processes perhaps from binding of native molecules to Aβ plaques and caging of label-free molecules, NADH and FAD, by the Aβ plaque formation as Alzheimer's disease sets in. This probable caging is also similar to three times longer lifetime observed for the triplet state of an encapsulated photosensitizer in a host/guest coordination

Table 2 Average fluorescence lifetime in AD tissue using single- and multi-photon excitation.

Molecule	Multi-photon	Excitation (nm)	Emission (nm)	t_1 (ps)	t_2 (ps)	a_1/a_2
NADH	1P	400	440	86.0	706.5	232.8
	2P	800	440	69	808	541
FAD	1P	400	530	95.7	722.3	122
	2P	800	530	63.5	513	1977
Tryptophan	3P	800	340	240	240	1

cage compared to its free analogue [28]. Recent work by our group using Terahertz time-domain spectroscopy also suggested similar isolation of tryptophan in AD tissue [29]. Three dominating absorption peaks associated to torsional–vibrational modes were observed in AD tissue, at about 1.44, 1.8, and 2.114 THz, closer to the peaks of free tryptophan molecules than in WT tissue. Our group has also reported from steady-state measurements larger quantum yield from tryptophan, NADH, and collagen in AD mouse brain tissues. The reduction in non-radiative energy transfer in the AD model due to probable caging is most likely responsible for such larger quantum yield [30].

The difference between the faster relaxation of two photon excitation fluorescence (2PEF) profile and that of 1PEF for the same photoexcitation is about 3.1 eV (excitation wavelengths are 800 nm and 400 nm, respectively, for 2PEF and 1 PEF). The following addresses the differences between the lifetimes in 2PE and 1PE transitions. The states excited in 1 PE require different parity states between ground and excited states while 2PE require same parity transition at a given photon energy. Parity can be even (+) and odd (−) states; (+) and (−) are different parity. In 1PE transitions from + to − state and from − to + state are both allowed by dipole transitions; while in 2PE transition molecule only goes from even to even state or from odd to odd state (each photon goes to a virtual state of opposite parity). So different states are excited in upper S_1 manifold. For example, 2PE transition starts from "+" and goes to "−" by 1PE transition to the virtual state, then the other 1PE goes from "−"to "+" state, giving total 2PE transition from + to − to + for 800 nm excitation.

On the other hand, when the excited state is pumped by 1PE for instance the 400 nm excites even to odd while 2PE at 800 nm ensures transition from even to even energy state in E vs. Q states manifold, 1PE and 2PE excite different energy states in the S_1 manifold so each has different k_r and k_{nr} to change emission fluorescence rates $k_f = k_r + k_{nr}$. This explains why the relaxation times are different in both AD and WT tissue. The different states in S_1 manifold are excited resulting in different emission lifetimes.

The relative isolation of the label-free molecules indicates the environmental changes inside the brain such as the deposition of amyloid-beta or tau plaques and neurofibrillary tangles-the telltale signs of AD. Time resolved energy transfer pathways will help define the mechanism for longer lifetime of key metabolic molecules in the brain.

5. Conclusion

It was shown experimentally by single- and multi-photon excitation that there exist large differences in fluorescence decay-times between AD and WT tissue in a mouse model. The differences exist for both emission bands of NADH and FAD. It is suggested that the environmental changes inside the brain, such as the deposition of amyloid-beta or tau plaques and neurofibrillary tangles, affect the native biomolecules leading to their relative isolation. Although further studies are needed for validating this assumption, these signature differences have great potential for non-invasive optical detection and imaging of AD. Furthermore, it has been shown the possibility of two- and three-photon time-resolved fluorescence imaging in brain is different. This ultrafast time resolved emission with single- and multi-photon absorption would lead to new approaches for understanding how metabolic pathways are affected in AD at the microscopic level.

Acknowledgements This research is supported in part by Corning, ARO, NIH grant 5SC1HD068129, and 2G12RR003060-26 A1 from the National Center for Research Resources.

References

[1] F. Hulstaert, K. Blennow, A. Ivanoiu, H. C. Schoonderwaldt, M. Riemenschneider, P. P. De Deyn, C. Bancher, P. Cras, J. Wiltfang, P. D. Mehta, K. Igbal, H. Pottel, E. Vanmechelen, and H. Vanderstichele, Neurology **52**, 1555–1562 (1999).
[2] R. R. Alfano, D. Tata, J. Cordero, P. Tomashefsky, F. Longo, and M. Alfano, IEEE J. Quantum Electron. **20**, 1507–1511 (1984).
[3] R. R. Alfano, B. B. Das, J. Cleary, R. Prudente, E. J. Celmer, Bull. N. Y. Acad. Med. **67**, 143–150 (1991).
[4] B. B. Das, F. Liu, and R. R. Alfano, Rep. Prog. Phys. **60**, 227–292 (1997).
[5] L. Marcu, P. M. W. French, and D. S. Elson (eds.), Fluorescence Lifetime Spectroscopy and Imaging: Principles and Applications in Biomedical Diagnostics, (CRC Press, Boca Raton, 2014).
[6] R. Cicchi, and F. S. Pavone, Anal. Bioanal. Chem. **400**, 2687–2697 (2011).
[7] E. Gulaj, K. Pawlak, B. Bien, and D. Pawlak, Adv. Med. Sci. **55**, 204–211 (2010).
[8] C. B. Pocernich and D. A. Butterfield, Neurotox. Res. **5**, 515–519 (2003).
[9] J. Hardy and D. J. Selkoe, Science **297**, 353–356 (2002).
[10] P. L. McGeer and E. G. McGeer, J. Neurovirol. **8**, 529–538 (2002).
[11] T. Wyss-Coray, Nat. Med **12**, 1005–1015 (2006).

[12] T. Kim, G. S. Vidal, M. Djurisic, C. M. William, M. E. Birnbaum, K. c. Garcia, B. T. Hyman, and C. J. Shatz, Science **341**, 1399–1404 (2013).
[13] P. Hartung, Laser Focus World **51**, 65–70 (2015).
[14] R. Ossenkoppele, W. J. Janse, G. D. Rabinovici, D. L. Knol, W. M. van der Flier, B. N. M. van Berckel, P. Scheltens, and P. J. Visser, JAMA **313**, 1939–1949 (2015).
[15] W. J. Jansen, R. Ossenkoppele, D. L. Knol, B. M. Tijms, P. Scheltens, F. R. J. Verhey, P. J. Visser, and Amyloid Biomarker Study Group, JAMA **313**, 1924–1938 (2015).
[16] W. E. Klunk, B. J. Lopresti, M. D. Ikonomovic, I. M. Lefterov, R. P. Koldamova, E. E. Abrahamson, M. L. Debnath, D. P. Holt, G. F. Huang, L. Shao, S. T. DeKosky, J. C. Price, and C. A. Mathis, J. Neurosci. **25**, 10598–10606 (2005).
[17] M. Koronyo-Hamaoui, Y. Koronyo, A. V. Ljubimov, C. A. Miller, M. K. Ko, K. L. Black, M. Schwartz, and D. L. Farkas, Neuroimage **54**, S204–S217 (2011).
[18] L. Shi, L. A. Sordillo, A. Rodríguez-Contreras, and R. R. Alfano, J. Biophotonics **9**, 38–43 (2016).
[19] F. T. Chan, G. S. Kaminski Schierle, J. R. Kumita, C. W. Bertoncini, C. M. Dobsonb and C. F. Kaminski, Analyst **138**, 2156–2162 (2013).
[20] S. Oddo, A. Caccamo, J. d. Shepherd, M. P. Murphy, T. E. Golde, R. Kayed, R. Metherate, M. P. Mattsom, Y. Akbari, and F. M. LaFerla, Neuron **39**, 409–421 (2003).
[21] L. Shi, A. Rodríguez-Contreras, and R. R. Alfano, J. Biomed. Opt. **19**, 126006 (2014).
[22] D. S. Correa, L. De Boni, L. Misoguti, I. Cohanoschi, F. E. Hernandez, and C. R. Mendonca, Opt. Commun. **277**, 440–445 (2007).
[23] S. R. Kantelhardt, J. Leppert, J. Krajewski, N. Petkus, E. Reusche, V. M. Tronnier, A. Giese, Neuro-Oncolo. **9**, 103–112 (2007).
[24] T. H. Chia, A. Williamson, D. D. Spencer, and M. J. Levene, Opt. Express **16**, 4237–4249 (2008).
[25] Y. Sun, N. Hatami, M. Yee, J. Phipps, D. Elson, F. Gorin, R. Schrot, and L. Marcu, J. Biomed. Opt. **15**, 056022 (2010).
[26] P. V. Butte, A. N. Mamelak, M. Nuno, S. I. Bannykh, K. L. Black, and Laura Marcu, *Neuroimage.* **54** (Suppl 1), S125–135 (2011).
[27] H. D. Viswasrao, A. A. Heikal, K. A. Kasischke, and W. W. Webb, J. Biol. Chem. **280**, 25119–25126 (2005).
[28] Y. Yang, J. Chen, J. Liu, G. Zhao, L. Liu, K. Han, T. R. Cook, and P. J. Stang, J. Phys. Chem. Lett. **6**, 1942–1947 (2015).
[29] L. Shi, P. Shumyatsky, A. Rodríguez-Contreras, and R. R. Alfano, J. Biomed. Opt. **21**, 15014 (2016).
[30] L. Shi, G. Harvey, T. Harvey, P. Marques, R. R. Alfano, and A. Rodrigues-Contreaus, Abstract 9703–29, *Photonic West – Optical Biopsy*, 124 (2016).

FULL ARTICLE

Time-resolved picosecond fluorescence spectroscopy with single- and multi-photon excitation was used to measure relaxation kinetics of key biomolecules in mouse brain in order to understand the energy flow pathways and develop a new diagnostic tool to detect Alzheimer's disease (AD). NADH and flavins showed longer fluorescence decays in AD than normal. The findings on time resolved energy kinetics of biomolecules in brain tissue of AD mouse model are presented for the first time.

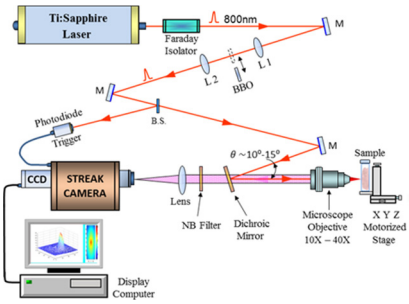

B. Das, L. Shi, Y. Budansky, A. Rodriguez-Contreras, R. Alfano*

1 – 8

Alzheimer mouse brain tissue measured by time resolved fluorescence spectroscopy using single- and multi-photon excitation of label free native molecules